CP violation in charm meson decays

Aleksei Chernov, on behalf of the LHCb collaboration
XXX Krakow Epiphany Conference, Young Scientists' Session

IFJ PAN, Krakow

Jan 11

Basics of CP symmetry violation

Three types of CP violation can be distinguished:

- *CP* violation in decay : $A_f = < f|\hat{H}|i > \neq \bar{A}_{\bar{f}} = < \bar{f}|\hat{H}|\bar{i} >$
  Measured through difference in partial decay widths (e.g for D^0):
  $A_{CP} = \frac{\Gamma(D^0 \to f) - \Gamma(\bar{D}^0 \to \bar{f})}{\Gamma(D^0 \to f) + \Gamma(\bar{D}^0 \to \bar{f})}$
- CP violation in mixing of neutral mesons (for example, $D^0 - \bar{D}^0$).
- CP violation in interference between mixing and decay: occurs when the same final state f is accessible for both flavours of a neutral meson.

This talk focuses on direct CPV in decays of D^0.

CP violation in charmed mesons

- Requires two amplitudes with different weak and strong phases
- Within SM, expected to be of the order $10^{-4} \div 10^{-3}$ (depending on penguin contribution). *JHEP12, 104 (2019)*

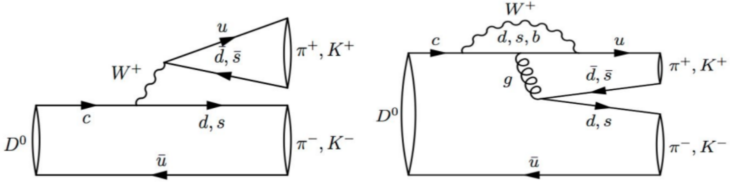

Example of a tree-level and one-loop (penguin) diagrams of $D^0 \to h^+ h^-$ decay.

$$A_{tree} \sim V_{u(d,s)} V^*_{c(d,s)} \sim \lambda \, (\lambda \approx 0.22)$$

$$A_b \sim \frac{m_b^2}{m_W^2} V_{ub} V^*_{cb} \sim \lambda^5 \, ; \; A_{sd} \sim \frac{m_s^2 - m_d^2}{m_W^2} (V_{us} V^*_{cs} - V_{ud} V^*_{cd})$$

Discovery of direct CPV in charm ΔA_{CP} PRL 122, 211803 (2019)

- Prompt $D^{*+} \to (D^0 \to h^+h^-)\pi^+_{tag}(+c.c)$ charm sample.
- Charge of $\pi^\pm_{tag}$ carries information about flavour of $D^0(\bar{D}^0)$
- Raw asymmetry measured by counting tags: $A_{raw} \equiv \frac{N_{D^0} - N_{\bar{D}^0}}{N_{D^0} + N_{\bar{D}^0}}$

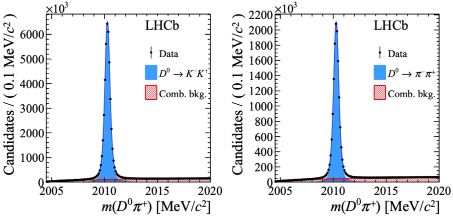

$$\Delta A_{CP} \equiv A_{CP}(K^+K^-) - A_{CP}(\pi^+\pi^-) \approx A_{raw}(K^+K^-) - A_{raw}(\pi^+\pi^-)$$

After combining prompt and secondary charm, Run1 and Run2 data:

$$\Delta A_{CP} = (-15.4 \pm 2.9) \times 10^{-4} \quad (5.3\sigma)$$

Nusiance asymmetries

$$A_{raw} = \frac{N_{D^0} - N_{\bar{D}^0}}{N_{D^0} + N_{\bar{D}^0}} \approx A_{CP} + A_{prod}(D^{*\pm}) + A_{det}$$

- Production asymmetry : $\sigma(pp \to D^{*+}X) \neq \sigma(pp \to D^{*-}X)$ (prompt)
- Detection asymmetry : difference in reconstruction efficiencies of h^+ and h^- with detector material and detector asymmetry. Driven mostly by tagging $\pi^{\pm}$.
- $A_{raw}(K^+K^-) - A_{raw}(\pi^+\pi^-) \approx \Delta A_{CP} + (A_{prod}(D^{*\pm}) - A_{prod}(D^{*\pm})) + (A_{det}(\pi^{\pm}_{tag}) - A_{det}(\pi^{\pm}_{tag}))$
- Price to pay: not sensitive to invidiual $A_{CP}(D^0 \to K^+K^-)$ and $A_{CP}(D^0 \to \pi^+\pi^-)$.

Disentangling $A_{CP}(K^+K^-)$ from ΔA_{CP}

- Use reference channels in order to extract $A_{CP}(K^+K^-)$ from A_{raw}.
- A_{prod} and A_{det} depend on the kinematics of conjugate particles - need to match signal and reference data. Overconstrain by using several reference channels.

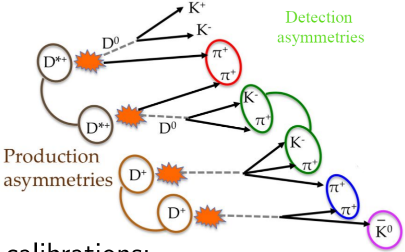

Two complementary calibrations:

- C_{D^+} : $A_{CP}(K^+K^-) = A_{raw}(D^0 \to K^+K^-) - A_{raw}(D^0 \to K^-\pi^+) + A_{raw}(D^+ \to K^-\pi^+\pi^+) - A_{raw}(D^+ \to \bar{K}^0\pi^+) + A_{CP}(\bar{K}^0)$
- $C_{D_s^+}$: $A_{CP}(K^+K^-) = A_{raw}(D^0 \to K^+K^-) - A_{raw}(D^0 \to K^-\pi^+) + A_{raw}(D_s^+ \to \phi\pi^+) - A_{raw}(D_s^+ \to \bar{K}^0K) + A_{CP}(\bar{K}^0)$

From ΔA_{CP} to invidual asymmetries in $D^0 \to h^+h^-$

PRL 131, 091802 (2023)

$A_{CP} \approx a^{dir}_{CP} - \frac{<t(f)>}{\tau(D^0)} A_\Gamma$ - substract residual mixing-related asymmetry.

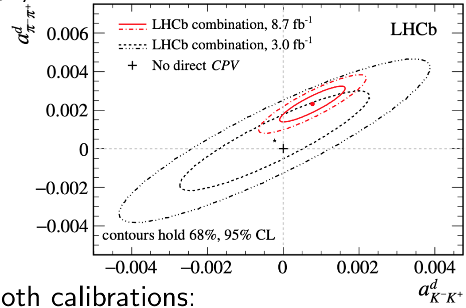

- Combining both calibrations: $A_{CP}(K^+K^-) = (6.8 \pm 5.4(stat.) \pm 1.6(sys.)) \times 10^{-4} \rightarrow$
- $\boldsymbol{a^{dir}_{KK} = 7.7 \pm 5.4 \times 10^{-4}}$. From this and ΔA_{CP} result:
- $a^{dir}_{\pi\pi} = 23.2 \pm 6.1 \times 10^{-4}$ - 3.8σ significance.
- $a^{dir}_{KK} + a^{dir}_{\pi\pi} = 30.8 \pm 11.4 \times 10^{-4}$ (2.7σ).

Radiative charm decays $D^0 \to V\gamma$

- $\boldsymbol{D^0 \to (\phi \to K^+K^-)\gamma}$, $\boldsymbol{D^0 \to (\rho^0 \to \pi^+\pi^-)\gamma}$, $\boldsymbol{D^0 \to (\bar{K}^{*0} \to K^-\pi^+)\gamma)}$ $+c.c$
- First observed at Belle (PRL 118, 051801 (2017)), A_{CP} consistent with null with % level uncertainties and decay rates $10^{-5} \div 10^{-4}$.
- SM predicts small $A_{CP} \sim 10^{-3}$, can be enhanced to % level by New Physics entering through the penguin contribution. (PRL 109, 171801 (2012), JHEP08, 091 (2017))
- $D^0 \to K^+K^-$ and $D^0 \to \pi^+\pi^-$ are used as reference channels to $D^0 \to \phi\gamma$ and $D^0 \to \rho\gamma$, correspondingly. Aim to measure $A_{CP}(D^0 \to V\gamma) - A_{CP}(h^+h^-) \approx A_{raw}(D^0 \to V\gamma) - A_{raw}(h^+h^-)$.

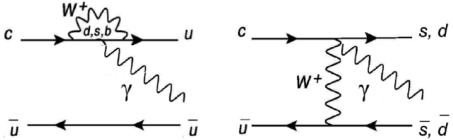

Penguin (left) and tree level (right) short-distance contributions to $D^0 \to \rho\gamma(\phi\gamma)$. ϕ penguin requires an extra vertex.

Main challenges in analysing $D^0 \to V\gamma$ decays at LHCb

Peaking backgrounds:

- Irreducible peaking background from $D^0 \to V\pi^0$; large decay rates $BR \sim 10^{-3} \to$ background-dominated sample.
- Subleading contriubtion from $D^0 \to V(\eta \to \gamma\gamma)$.

Particle reconstruction:

- Relatively soft photons: $p_T(\gamma) \sim GeV \to$ limited resolution, signficiant combinatorial background;
- Calorimeter-only reconstruction (the only possibility for γ/π^0 in the final state) results in worse invariant mass resolution compared to tracks.
- $\pi^0 \to \gamma\gamma$ - can be merged ($\gamma\gamma$ reconstructed as γ) or resolved - 2 separate γ clusters. If one photon is not reconstructed, resolved π^0 contributes as well.

$D^0 \to \bar{K}^{*0}\gamma$ toy sample; signal suppressed region

- Pseudo-data based on Run 1 $D^{*+} \to (D^0 \to V\gamma)\pi^+_{tag}(+c.c)$ LHCb data. Resolved π^0 background suppressed by π^0 veto, merged - by MVA tool based on calorimeter observables (IsPhoton). $p_T(\gamma) > 2\ GeV$.
- Separate residual π^0 background by using helicity angle θ of the V meson.
- Use signal-suppressed region of $\cos(\theta)$ observable to calibrate MC-based PDFs for peaking backgrounds.

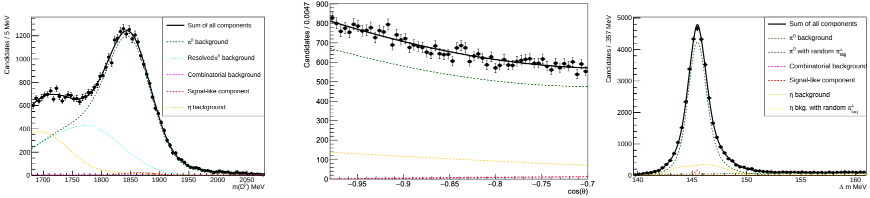

Unbinned ML multidimensional fit to the toy distribution based on the combined sample of π^+ and π^- tagged decays of $D^0 \to \bar{K}^{*0}\gamma$. $N_{evt} = 40000$.

$D^0 \to \bar{K}^{*0}\gamma$ sample; signal region

- Parameters for peaking backgrounds PDFs fixed to values obtained from calibration fit.
- Overall signal fraction $\sim 7\%$.

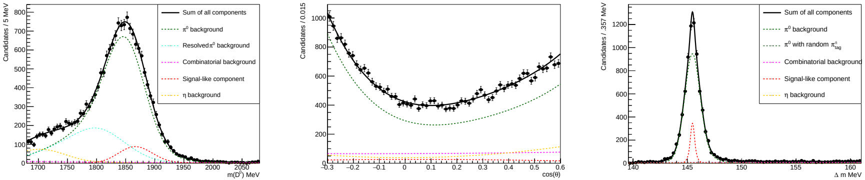

Unbinned ML multidimensional fit to the toy distribution based on the combined sample of π^+ and π^- tagged decays of $D^0 \to \bar{K}^{*0}\gamma$. $m(D^0)$ is shown in the $3\sigma_{avg}$ range from signal peak in Δm and vice versa. Helicity angle distribution is shown in full $(m(D^0), \Delta m)$ range. $N_{evt} = 33000$.

Summary and outlook

- Direct CPV in charmed mesons discovered at LHCb in 2019
  $\Delta A_{CP} = (-15.4 \pm 2.9) \times 10^{-4} \quad (5.3\sigma)$
- First evidence for direct CPV in invidiual decay found in 2023
  $a^{dir}_{\pi\pi} = 23.2 \pm 6.1 \times 10^{-4} \quad (3.8\sigma)$
- Direct CPV is expected to differ for different decay channels, and for many other D and D_s decays consistent with zero. More precise measurements and more statistics expected to bring a clearer picture.
- First measurement of CPV in radiative charm decays with LHCb is ongoing.

Discriminating observable - Helicity angle

- Helicity angle θ defined as an angle between momenta of h^- and D^0 in the rest frame of V (+c.c)

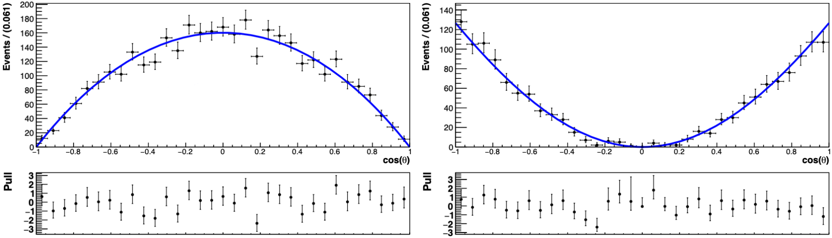

Distributions of cos(θ) observable of $D^0 \to \phi\gamma$ (left) and $D^0 \to \phi\pi^0$ background (right), using simulated 2012 data. Overlaid PDFs are $sin^2\theta$ and $\cos^2\theta$, respectively, adjusted by a small correction due to detector acceptance effects.

- Signal suppressed ($\cos\theta \sim \pm 1$) and signal enhanced ($\cos\theta \approx 0$) regions.

Fit to $D^0 \rightarrow KK$ reference sample wit kinematic weights

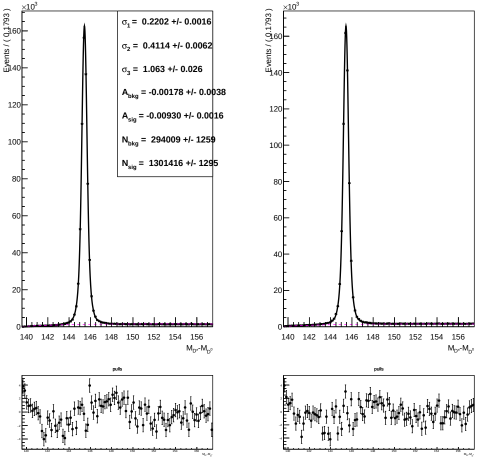

Unbinned maximum likelihood simulatenous fit to π^+ and π^- tagged subsamples using observable $\Delta M \equiv M(D^{*+} - M(D^0))$ in the weighed $D^0 \rightarrow KK$ 2012 data. Christoph Lagenbruch's approach to calculating uncertainties of the fit parameters in weighed datasets is used.